SOILS AND FOUNDATIONS Vol. 41, No. 6, 1-16, Dec. 2001
Japanese Geotechnical Society

PREDICTION OF THE PERFORMANCE OF A GEOGRID-REINFORCED SLOPE FOUNDED ON SOLID WASTE

JORGE G. ZORNBERG[i] and EDWARD KAVAZANJIAN JR.[ii]

ABSTRACT

An investigation was undertaken to evaluate the integrity of a geogrid-reinforced steep slope subjected to significant differential settlements and seismic loading. The reinforced soil structure under investigation was constructed in 1987 in order to enhance the stability of steep landfill slopes at the Operating Industries, Inc. (OII) Superfund site, a hazardous waste site in southern California. The site is in an area of high seismicity. The 4.60 m high, 460 m long geogrid-reinforced structure was founded, along most of its length, on concrete piers located towards the front of the structure. However, as the back of the reinforced slope was founded on waste, the structure experienced more than 600 mm of differential settlements ten years after its construction. A geogrid experimental testing program was implemented to evaluate the performance of the reinforcements when loaded rapidly after a period of constant load. A finite element numerical simulation was performed to assess the integrity of the geogrid reinforcements when subjected to 30 years of additional differential settlements followed by the design earthquake. The maximum geogrid strains predicted for a sequence of expected static and extreme seismic loadings were found to be well below the geogrid allowable strain values, indicating that the integrity of the structure should be maintained even when subjected to large differential settlements and severe earthquake loads. The numerical results show that the critical reinforced zone (i.e., the reinforcement layers that are strained the most) that corresponds to different loading mechanisms (construction, differential settlement, seismic loading) occurs at different elevations within the reinforced soil structure.

Key words: case histories, differential settlements, finite element analysis, geogrids, geosynthetics, landfills, seismic design, soil reinforcement, steep slope (**IGC**: B3/E6/H2).

INTRODUCTION

A geogrid-reinforced toe buttress was constructed under the direction of the United States Environmental Protection Agency (EPA) in order to enhance the stability of steep landfill slopes at the Operating Industries, Inc. (OII) Superfund site, a hazardous waste site in southern California. The OII landfill is located approximately 16 km east of downtown Los Angeles, in an area of high seismicity. The 4.60 m high, 460 m long toe buttress was constructed in 1987 immediately adjacent to residential developments. The waste slopes behind the toe buttress at the time of this investigation were up to 37 m high, with intermediate slopes between benches up to 18 m high and as steep as 1.3H:1V (horizontal:vertical). The geogrid-reinforced structure was founded, along most of its length, on concrete piers located towards the front of the structure. However, as the back of the reinforced structure was founded on waste, the toe buttress experienced significant differential settlements since its construction. A thorough evaluation was then undertaken as part of predesign studies for landfill closure to assess the long-term static and seismic integrity of the reinforced toe buttress and, consequently, the stability of the landfill slopes behind the structure. The analyses presented in this paper provided evaluation of the future performance of the structure considering 30 years of additional settlements followed by the design earthquake.

As an existing structure at the OII Landfill Superfund site, the geogrid-reinforced toe buttress could only become an integral component of the final closure system if its long-term and seismic performance was adequately demonstrated. The major challenge in this demonstration was the prediction of the geogrid strains for internal stability assessment of the structure. This paper documents the experimental and analytical studies undertaken to predict the geogrid strains of this structure and, more generically, to understand the development of geogrid strains within structures subjected to multiple loading conditions. This case history is a good example of a project in which nonconventional tests (of geogrids and solid waste) and finite element analyses provided key insight in support of the design of a hazardous waste closure system.

[i] Assistant Professor, Department of Civil Environmental and Architectural Engineering, University of Colorado at Boulder.
[ii] Principal, GeoSyntec Consultants, Huntington Beach, California.
Manuscript was received for review on June 5, 2000.
Written discussions on this paper should be submitted before July 1, 2002 to the Japanese Geotechnical Society, Sugayama Bldg. 4F, Kanda Awaji-cho 2-23, Chiyoda-ku, Tokyo 101-0063, Japan. Upon request the closing date may be extended one month.

Even though instrumented full-scale structures have been useful to understand the development of reinforcement strains induced by construction loads, very little is known about the development of reinforcement strains induced by differential settlements and by seismic loads. By evaluating the OII case history, this investigation also provides insight into the performance of geosynthetic-reinforced soil structures subjected to a combination of different long-term static and seismic loading mechanisms.

BACKGROUND AND COMPONENTS OF THIS INVESTIGATION

Current understanding on the strain distribution within geosynthetic-reinforced soil structures is mainly based on the information gathered from structures subjected to vertical loading. Instrumentation monitoring and numerical simulations have documented the performance of reinforced soil structures subjected to selfweight loads induced during construction (e.g., Tatsuoka et al., 1990; Christopher et al., 1994; Zornberg and Mitchell, 1994; Rowe and Ho, 1997). However, little experience has been reported on the post-construction performance of reinforced soil structures subjected to differential settlements and seismic loading. The analyses presented herein provide insight on the development of reinforcement strains induced by loads other than selfweight in geosynthetic-reinforced soil structures.

Only a few case histories have been reported on the performance of reinforced soil structures subjected to differential settlements. Most of these cases refer to structures built using rigid facing and inextensible inclusions, in which reinforcement strains have been induced by differential settlements between the backfill and the wall facing (Chang and Forsyth, 1977; Bathurst et al., 1988; Blight and Dane, 1989). Case histories reporting the performance of geosynthetic-reinforced soil structures subjected to significant differential settlements are very limited. A design effort was reported regarding provisions taken to address potential differential settlements of a geotextile-reinforced wall (Stevens and Souiedan, 1990). The wall design accounted for differential settlements of up to 250 mm between a portion of the wall founded on a pile cap and the remainder of the wall bearing directly on the ground. Specifically, the design incorporated a vertical offset in the geotextiles so that no tension in the reinforcements would occur by expected differential settlements.

Although displacement-based approaches have already been proposed for seismic design of reinforced soil structures, current design practice is still typically based on pseudo-static approaches. The magnitude of the pseudo-static thrust on retaining walls is generally estimated using the Mononobe-Okabe approach (Kramer, 1996). This pseudo-static approach has been extended to the design of reinforced soil walls (e.g., Elias and Christopher, 1997). Conventional seismic design methods for unreinforced soil slopes have also been extended to the design of reinforced soil slopes using pseudo-static limit equilibrium models (e.g., Bonaparte et al., 1986). Because of their comparatively high flexibility, the performance of geosynthetic-reinforced soil structures during earthquakes has been excellent (e.g., Tatsuoka et al., 1998). Qualitative field assessments have been reported on the seismic performance of reinforced soil structures subjected to earthquake loads during the 1989 Loma Prieta (San Francisco) earthquake (Collin et al., 1992), the 1994 Northridge (Los Angeles) earthquake (Sandri, 1994; Stewart et al., 1994; White, 1996), and the 1995 Great Hanshin (Kobe) earthquake (Tatsuoka et al., 1996). Because of the comparatively high intensity of the ground motions, the behavior of reinforced soil structures during the 1995 Kobe Earthquake is particularly noteworthy. During this seismic event, satisfactory performance was observed in more than 2 km of geogrid-reinforced soil retaining walls with full height rigid facing. This is particularly relevant considering that damage to many new wooden houses, concrete retaining walls, and reinforced concrete buildings in the nearby area was particularly severe. Possibly the only documented failure of reinforced soil structures attributed to earthquake loading occurred during the 1999 Chi-Chi (Taiwan) earthquake (Huang, 2000; Huang and Tatsuoka, 2001). The structures, located near the National Chi-Nan University, were subjected to an estimated peak acceleration of 0.45 g. Although the causes of the failure are still under investigation, it appears that factors other than internal stability (e.g., failure of the underlying foundation) may have led to the collapse. With the exception of this recent incident in Taiwan, qualitative evaluations have generally indicated an excellent seismic performance of geosynthetic-reinforced soil structures. However, there is still little quantitative information regarding the distribution and magnitude of seismically induced strains in geosynthetic reinforcements.

Considering the lack of quantitative information regarding the development of strains within reinforced soil structures subjected to differential settlements and earthquake loading, a significant effort was undertaken as part of this investigation to provide such information. To this effect, the analyses undertaken to evaluate the future performance of the toe buttress at the OII Landfill Superfund site included three distinct components:

a) *Evaluation of field conditions and material properties*. This included interpretation of monitoring data to assess the history of differential settlements and to predict future differential settlements in the toe buttress area. In addition, information on the relevant geogrid, backfill, solid waste, and foundation properties was compiled for use in the analyses. This included an experimental testing program implemented to evaluate the performance of the reinforcements when loaded rapidly after a period of constant load.

b) *Evaluation of the stability of the southeastern landfill slopes using limit equilibrium*. These analyses addressed global stability of the steep landfill slopes behind the toe buttress, assuming that differential settlement

and/or earthquake loads do not compromise the internal integrity of the toe buttress.

c) *Evaluation of the internal integrity of the geogrid-reinforced toe buttress using nonlinear finite element analysis*. Analyses were performed to predict the geogrid strains induced within the toe buttress by long-term differential settlements followed by the design earthquake. The finite element analyses were performed using a large displacement approach. Specifically, the numerical investigation simulated the development of geogrid strains induced by: (i) toe buttress construction, (ii) gradual increase in differential settlements, and (iii) earthquake loading.

The investigation of the integrity of the reinforced toe buttress was undertaken as part of compliance pre-design analyses for the final closure system at the site. A description of the several investigations that evaluated the seismic performance of the OII Landfill Superfund site, including an overview of the toe buttress investigation, are presented elsewhere (GeoSyntec Consultants, 1996; Zornberg and Kavazanjian, 1998; Matasovic and Kavazanjian, 1998; Morochnik et al., 1998; Augello et al., 1998).

SITE DESCRIPTION

Toe Buttress Information

The OII Landfill Superfund site is located in the city of Monterey Park and the adjacent city of Montebello, California, approximately 16 km east of downtown Los Angeles (Fig. 1(a)). The landfill property is divided by California State Highway 60 (the Pomona Freeway) into a 18-hectare, comparatively flat, North Parcel and a 59-hectare South Parcel where most of the landfilling occurred (Fig. 1(b)). The refuse mass in the South Parcel rises to a height of over 76 m above grade with slopes as steep as 1.3H:1V (Fig. 1(c)). The South Parcel was formerly a sand and gravel quarry pit cut into the Montebello Hills. The quarry pit, up to 60 m deep in places, was filled with solid waste over a 40-year period. The site accepted residential, commercial, and industrial solid wastes. In addition, particularly at the west portion of the South Parcel, the landfill accepted liquid wastes. There is no evidence indicating that subgrade preparation or installation of a liner system took place prior to the placement of solid waste fill in the quarry.

The maximum vertical thickness of the solid waste in the South Parcel is approximately 100 m. The landfill

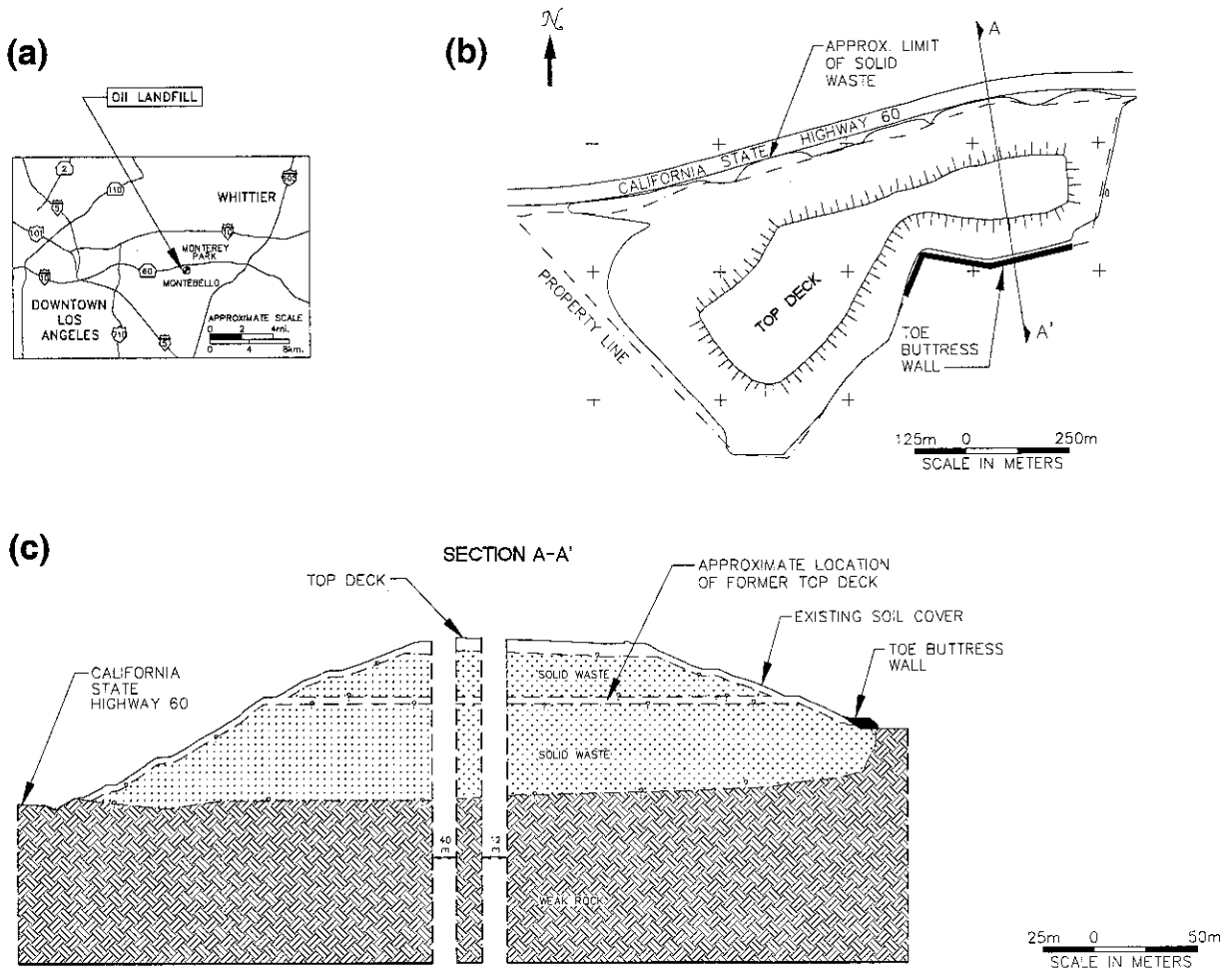

Fig. 1. OII Superfund Landfill: (a) site location, (b) plan view of the South Parcel, (c) vertical cross-section of the landfill showing the toe buttress wall

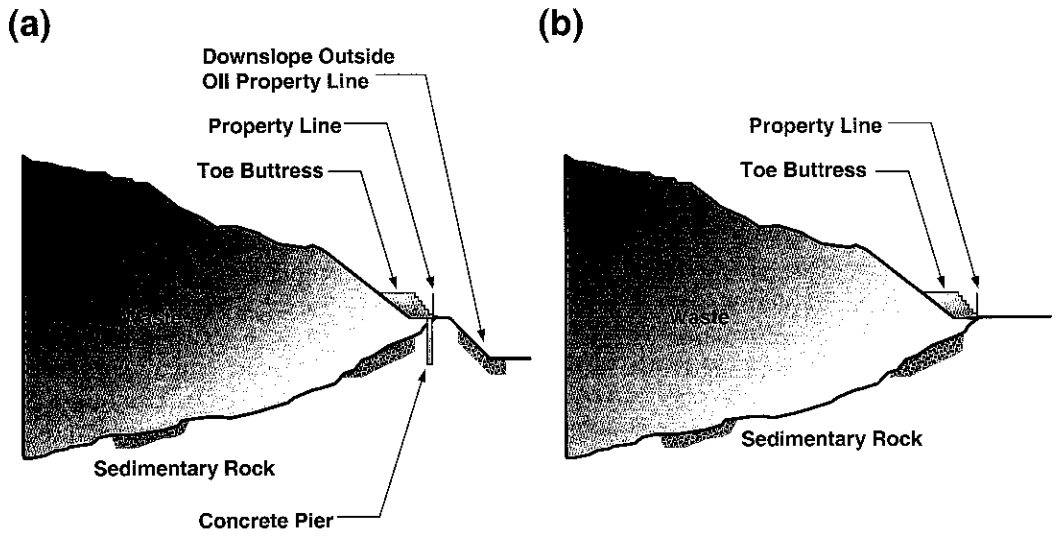

Fig. 2. Typical profiles of the toe buttress at the OII Superfund Landfill: (a) profile with concrete piers, (b) profile without concrete piers

received waste until 1984. An interim soil cover of variable thickness (1 to 5 m), consisting of silty clay to silty sand, was then placed on top of the landfill. The South Parcel has been undergoing final closure under the EPA Superfund program since 1985. Instrumentation and monitoring of the landfill was initiated at that time, along with a variety of site characterization and pre-design analytical studies.

The approximately 4.6 m high, 460 m long toe buttress was constructed in 1987 under the direction of EPA as an emergency measure in response to observed slope movements in this area. Several alternative remedial measures were evaluated to provide additional stability to the southeastern landfill slopes (Woodward Clyde Consultants, 1986). The toe buttress was selected at the time as the most feasible alternative to enhance the stability in this area of the landfill. Schematic profiles through the toe buttress and the waste slope along the southeastern perimeter of the OII Landfill are illustrated in Fig. 2. Reinforced cast-in-place concrete piers were constructed, along the original roadway located at the toe of the landfill, in areas where the natural ground surface continued to slope downward beyond the property line (Fig. 2(a)). Piers were not installed in areas where the ground surface was level beyond the toe of the waste slope (Fig. 2(b)). A total of 201 piers, 0.9-m in diameter, were installed at 1.8-m center to center spacing along approximately 360 m of the 460 m long toe buttress. The length of the piers ranged from 4.9 to 7.3 m.

The toe buttress was constructed using HDPE geogrid reinforcements, which were installed using a wrap-around procedure. Sandy gravel was used as backfill soil. Reinforcement length was typically 4.3 m and spacing between primary reinforcement layers was 0.9 m. An additional 2.1 m long intermediate geogrid was placed at mid-height between primary reinforcement levels.

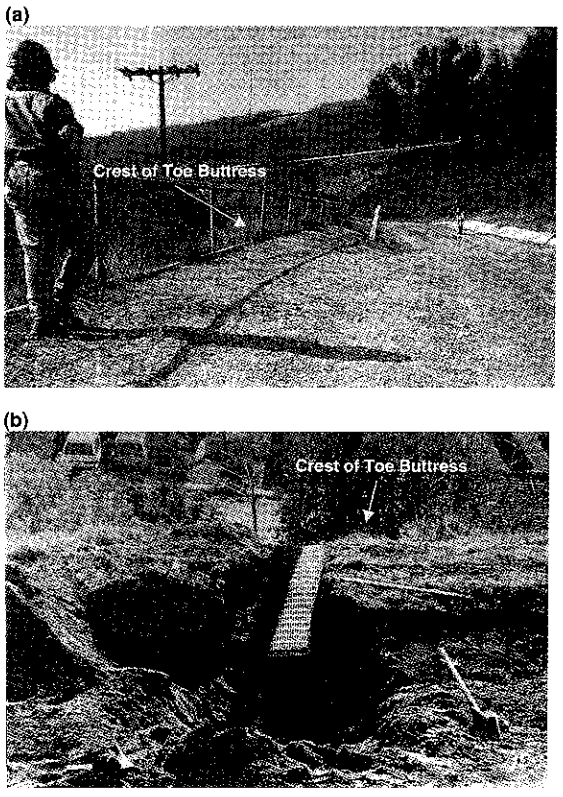

Fig. 3. View of the differential settlements across the toe buttress at the OII Superfund Landfill: (a) surface view (October 1995), (b) exposed top geogrid layer

Toe Buttress Deformations

Significant differential settlements have taken place over the width of the toe buttress since its construction along most of its alignment, as indicated by visual observations and survey data. The presence of the concrete piers under the front edge of the buttress and the thickness of the waste increasing towards the back of the buttress contributed to the observed differential settlements.

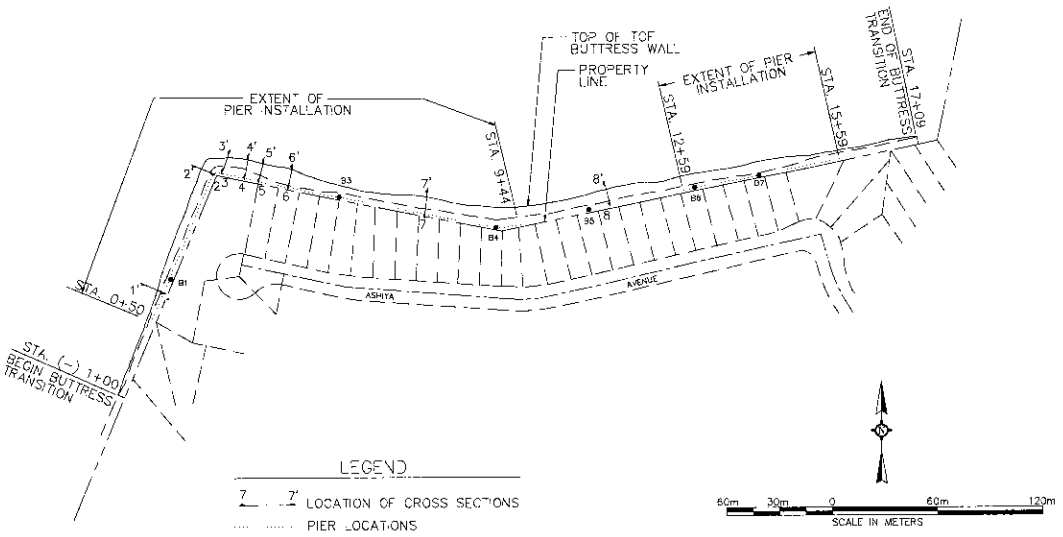

Fig. 4. Plan view of the toe buttress area showing location of monitored cross-sections

Table 1. Summary of differential settlements at the back of the toe buttress

	Differential settlements for period 1987–1992 (mm)	Differential settlements for period 1992–1996 (mm)
Cross-section 1-1'	146	192
Cross-section 2-2'	439	73
Cross-section 3-3'	421	387
Cross-section 4-4'	719	113
Cross-section 5-5'	841	−46
Cross-section 6-6'	488	171
Cross-section 7-7'	415	15
Cross-section 8-8'	235	−27
Average of 8 sections for the entire period	463	110
Average of 8 sections per year	82	30

Figure 3(a) shows a view of the differential settlements at toe buttress as of October 1995. The considerable tilting of the posts protecting a monitoring well is good evidence of the significant differential settlements. An eloquent view of the major differential settlements in the area is also shown in Fig. 3(b), which depicts the significant inclination of the geogrids, revealed after exposing the top reinforcement layer. It should be emphasized that, following conventional construction procedures, the geogrid layers had been placed horizontally during construction of the toe buttress in 1987.

Settlement profiles at eight locations along the top of the toe buttress (Fig. 4) were measured in October 1992 and in April 1996. The results from the 1996 survey showed that differential movements were still occurring. However, the rate of differential settlements at most of the stations along the toe buttress had decreased since 1992. Table 1 summarizes the differential settlement monitored at the eight cross sections between the crest of the toe buttress and a concrete drainage ditch located at the back of the structure. The average differential settlement monitored at the eight cross sections is 463 mm for the period March 1987-October 1992 (5.6 years), which corresponds to a differential settlement rate of 82 mm per year. For the period October 1992-April 1996 (3.5 years), the average differential settlement is 110 mm, which corresponds to a differential settlement rate of 30 mm per year. It should be noted, however, that the settlement rate varied for the different cross sections.

The settlements monitored at the back of the toe buttress for each individual cross section were projected forward in time as a straight line on a semi-logarithmic plot to evaluate the potential future settlements (Fig. 5). Because the settlement surveys were not tied to an external reference, a fixed elevation was assumed for the toe buttress surface immediately above the drilled piers. With the exception of Cross Section 3, the differential settlement projected 40 years beyond the end of construction (until year 2027) was less than 1170 mm. The projected differential settlement for Cross Section 3 was 1980 mm. However, discrepancies between the reported survey results and deformations monitored in a monitoring well located at this cross section (Fig. 3(a)) suggest that the actual differential settlements at this cross section should be smaller than those reported in Table 1. Because of the inconsistency of the data for Cross Section 3, the projected

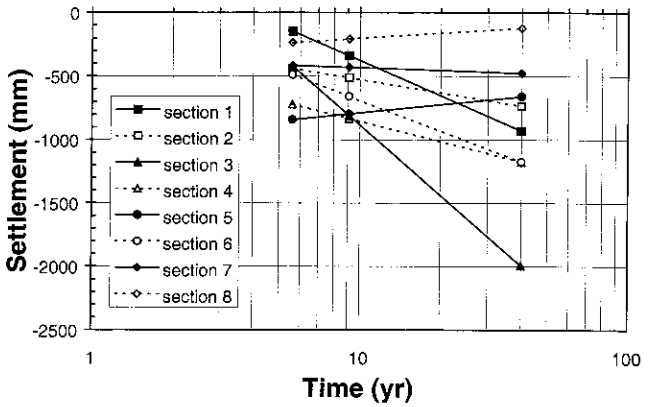

Fig. 5. Monitored differential settlements at the eight cross sections (Note: Settlements at year 40 are projected values)

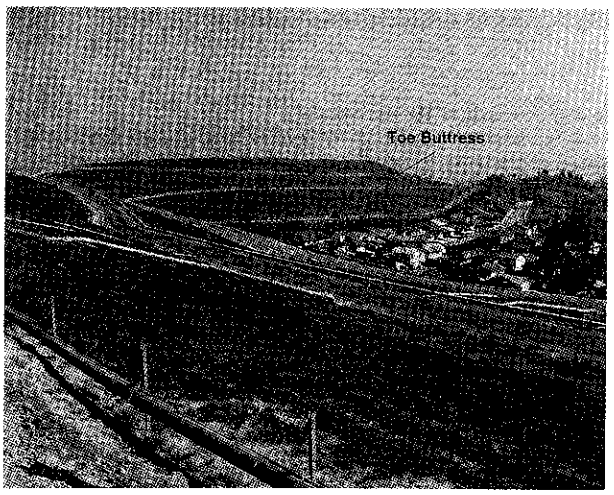

Fig. 6. View of the southeastern portion of the OII Superfund Landfill after construction of the final cover system (September 1999)

differential settlement of 1980 mm for this section was treated as an outlier. A differential settlement of 1170 mm was considered a conservative projection over the next 30 years of the expected differential settlements for the purpose of evaluating the long-term integrity of the toe buttress. Nonetheless, the performance of the toe buttress when subjected to a projected differential settlement of 1980 mm was also evaluated.

The design of the final cover was completed in 1998. Final design includes an evapotranspirative soil cover (Zornberg and Caldwell, 1998) and enhancement of the surface water, leachate, and gas control systems. Figure 6 shows the recently constructed (March 2000) cover system in the vicinity of the toe buttress area. As shown in the figure, the southeastern boundary of the landfill shown is immediately adjacent to the backyard of residences. The pre-existing geogrid-reinforced toe buttress could only be integrated into the final closure system because its performance was shown to be adequate, as documented in this paper, under additional differential settlements and seismic loads.

Bottom of the Waste Geometry

An assessment of the available information on the geometry bottom of the waste beneath the toe buttress was undertaken to aid in the toe buttress global stability evaluation. The logs for the 201 concrete piers drilled along the toe buttress, along with historical aerial photos and data from borings through the waste, provided relevant information regarding the depth of the waste in the toe buttress area. This information indicated that the bottom of the waste in the vicinity of the toe buttress area slopes down into the landfill, as schematically illustrated in Fig. 2, at an inclination of approximately 45° from the property line.

MATERIAL PROPERTIES

Geogrid Properties

The toe buttress was constructed using HDPE geogrid reinforcements manufactured in the 80's by the Tensar Corporation (SR2 geogrids). Although manufacturing of this reinforcement product had been discontinued by the time of this investigation, some of the geogrid properties needed for the analyses undertaken in this study were obtained from information available from the literature. This available information was supplemented with tests performed on archived geogrid samples provided by the geogrid manufacturer. Available technical information indicated that a 10% limiting strain was a conservative estimate of the geogrid allowable strain for long-term static loading (Bonaparte and Berg, 1987). Also, available information indicated that 20% was an adequate geogrid allowable strain for rapid (seismic) loading (McGown et al., 1984).

Tensile strength properties of the geogrid reinforcements were required as input information for the limit equilibrium analyses performed in this study. The long-term allowable design tensile strength, as recommended by the manufacturer for the geogrid used in toe buttress, is 29.2 kN/m. This long-term allowable design strength is based upon the results of long-term (10,000 hours minimum) constant-load creep tests extrapolated to a design life of 120 years. This tensile strength value was used for long-term static analyses. The current state-of-practice for selection of long-term allowable reinforcement tension is to obtain the tension-strain from tensile tests such as the wide-width tensile test (ASTM D 4595) and then to reduce the results to account for creep. The geogrid has a longitudinal (machine direction) wide-width tensile strength of 78 kN/m (Bonaparte and Berg, 1987). Wide-width tensile strength is then more than 2.5 times higher than the creep limited long-term allowable strength used in the static stability evaluation. Wide-width test results were used in this study to characterize the geogrid tensile strength under rapid (seismic) loading conditions.

Tensile load-strain properties of the geogrid reinforcements are required as input information for the finite element analysis performed in this study. Bonaparte and Berg (1987) evaluated the long-term allowable tension of SR2 geogrids using the isochronous reinforcement ten-

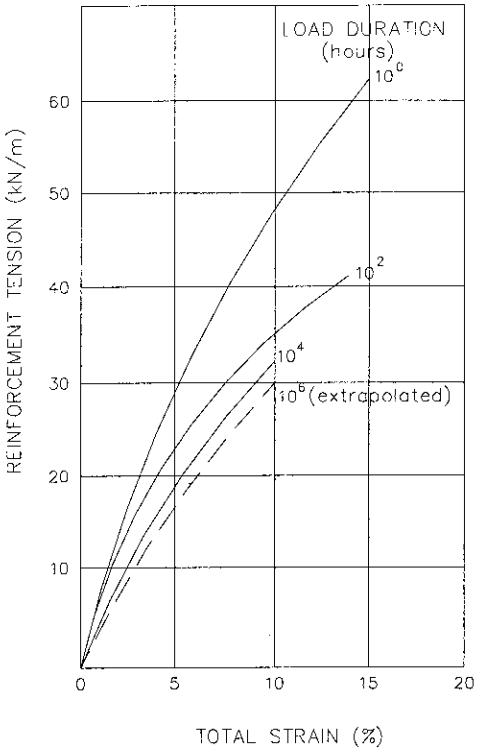

Fig. 7. Isochronous load-strain curves for SR2 geogrid (after Bonaparte and Berg, 1987)

sion versus strain curves illustrated in Fig. 7. The isochronous load-strain curves in the figure were obtained from constant-load creep tests. The curve for load duration of 10^6 hours (11 years) was used in the finite element analyses of the toe buttress wall to define the geogrid stiffness under static loading conditions. A geogrid stiffness of 300 kN/m was determined using a strain of 10% in the reinforcement. The curve for load duration of 10^0 hours (i.e. 1 hour) was used to define the geogrid stiffness for conditions representative of rapid (seismic) loading. A geogrid stiffness of 425 kN/m was determined in this case.

An experimental testing program was performed as part of this investigation to complement reported information on the geogrid mechanical properties. The testing program included wide-width tensile tests and creep tests followed by rapid loading to failure. The main objective of this testing program was to address EPA concerns that sudden loading after an extended period of creep could potentially reduce the geogrid allowable strain (or the geogrid ultimate tensile strength) to values less than those obtained from wide-width testing. Specifically, the experimental testing program evaluated the mechanical behavior of archived geogrid specimens for the case of combined static and rapid (seismic) loading. The testing program included the following:

- wide-width tensile tests performed at 10%/min strain rate;
- wide-width tensile tests performed at 2%/min strain rate;
- 100 hr. creep test followed by loading at 10%/min strain rate; and
- 100 hr. creep test followed by loading at 2%/min strain rate.

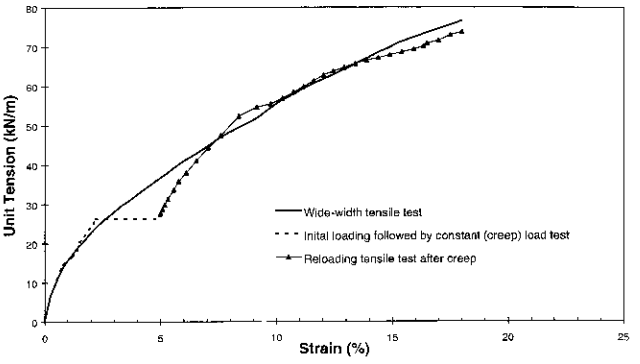

Fig. 8. Results of geogrid tests performed at 10%/min strain rate

Consistent with conventional wide-width tensile testing (ASTM D 4595), tests were performed using a strain rate of 10%/min. In addition, and in order to evaluate the potential effect of strain rate in the post-creep reloading test results, the program incorporated testing using a strain rate of 2%/min. The loading history of the tree-stage tests included an initial rapid loading, constant load (creep), and rapid post-creep reloading. Initial loading was performed at a strain rate of approximately 10%/min. The constant-load (creep) portion of the tests was performed at a constant tensile load of 26.3 kN/m, which corresponds to 90% of the reported long-term design strength of the geogrid. This comparatively high constant tensile load was selected in order to emphasize the potential effect of creep on the results obtained during the third (rapid reloading) stage. The rapid post-creep reloading portion of the tests was conducted until tensile failure.

Figure 8 summarizes the results of laboratory tests performed on geogrids using a 10%/min strain rate loading. The averaged test results of three wide-width tensile tests (i.e., rapid loading) define a control curve that is compared to test results obtained by the three-stage test. As observed in the figure, during the rapid reloading that followed the 100-hr. creep loading period, the geogrid shows an initially higher stiffness than the one observed in the wide-width (control) test at an equivalent tensile load. In fact, the geogrid stiffness during rapid reloading is similar to the geogrid stiffness during initial loading. However, the post-creep reloading portion of the test eventually matches the wide-width (control) curve. Both the wide-width (control) curve and the creep/reloading curve fail at approximately the same ultimate tensile strength and show a similar strain level at failure. The pattern of behavior observed in geogrids subjected to rapid loading following a constant loading period resembles that observed for the case of clay soils (Kavazanjian and Mitchell, 1980).

Figure 9 summarizes the results of geogrid tests performed using a strain rate loading of 2%/min. Initial loading up to the 26.3 kN/m was performed at a strain

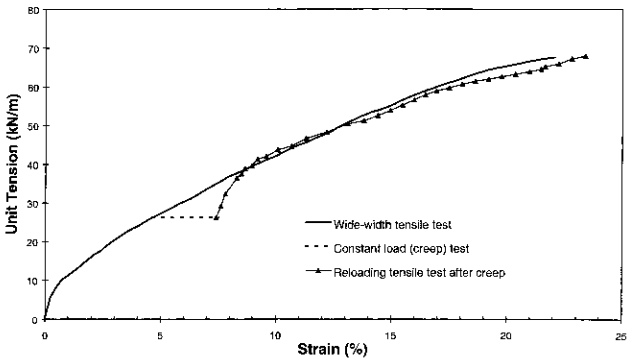

Fig. 9. Results of geogrid tests performed at 2%/min strain rate

rate of approximately 10% rather than 2%/min. Consequently, in order to compare the two sets of tests, the constant-load creep portion of the creep/reloading curve was shifted so that the strain level at the beginning of creep loading matches the wide-width (control) curve. Also in this case, the geogrid shows a comparatively higher stiffness during reloading (following the 100 hr. creep loading period) than the one observed in the control curve at an equivalent tensile load. The post-creep reloading portion of the test eventually matches the wide-width (control) curve.

By showing that rapid loading following creep should not reduce the allowable tensile strain in the geogrid reinforcement, the geogrid testing program addressed concerns regarding the post-creep performance of the reinforcements. This observation appears to be valid for different loading strain rates. Also, the results of the testing program on archived samples verified that a geogrid allowable strain of 20% was appropriate for the case of static creep followed by rapid seismic loading.

Backfill, Waste, and Foundation Soil Properties

The backfill material used during construction of the toe buttress fill is a sandy gravel classified as GP using the Unified Soil Classification System. Backfill specifications required a minimum relative compaction of 95%, based on modified Proctor compaction test, except within 0.61 m of the toe buttress face. The constitutive relationship used in the finite element analyses to model the stress-strain-strength behavior of the backfill is the hyperbolic model proposed by Duncan et al. (1980). Hyperbolic model parameters for the backfill were obtained from triaxial test results reported for a sandy gravel of similar grain size distribution and compaction characteristics (Zornberg and Mitchell, 1994). The hyperbolic parameters selected for the gravel backfill are shown in Table 2.

Field sampling and laboratory testing programs were undertaken as part of a comprehensive investigation aimed at characterizing the mechanical properties of the solid waste material under both static and dynamic loading (GeoSyntec, 1996). The experimental testing program of the solid waste material included visual classification, moisture content determination, one-dimensional compression tests, direct shear tests, static and cyclic simple shear tests, and shear wave velocity measurements. Results from the direct shear tests performed as part of the experimental testing program were used in this study to define the waste shear strength properties needed for limit equilibrium and finite element analyses of the toe buttress. Triaxial compression tests on solid waste material were not available. However, results from the cyclic simple shear tests were used, as explained below, to define some of hyperbolic parameters needed to characterize the stress-strain behavior of the solid waste material. The direct shear and simple shear tests were performed using 457 mm diameter reconstituted specimens of waste material excavated from the landfill. The variation of the initial tangent Young's modulus, E_i, with confining pressure is defined using the hyperbolic model as (Duncan et al., 1980):

$$E_i = K P_a(\sigma_3/P_a)^n \quad (1)$$

where K and n are hyperbolic model parameters, σ_3 is the effective confining pressure, and P_a is the atmospheric pressure. Figure 10 shows initial Young's modulus obtained from cyclic simple shear tests performed as part of the waste testing program. The modulus values are plotted versus the effective confining pressure on a log-log scale. For purposes of defining the hyperbolic parameters, the initial modulus was defined as the modulus corresponding to a shear strain of 0.2%. The figure shows that, as in the case of soils, the relationship between initial modulus and confining pressure of waste is well represented by a linear relationship on a log-log

Table 2. Hyperbolic soil parameters for the backfill and waste materials

Parameter	Parameter definition	Backfill	Waste
K	Young's modulus coefficient	913.00	212.00
n	Young's modulus exponent	0.60	0.61
R_f	Failure ratio	0.64	0.70
c (kPa)	Cohesion	0.00	28.70
ϕ_0 (°)	Friction angle at 1 atm.	46.10	31.00
$\Delta\phi$ (°)	Friction angle reduction parameters	5.30	0.00
K_B	Bulk modulus number	250.00	212.00
m	Bulk modulus exponent	0.80	0.61
K_{ur}	Unload-reload modulus coefficient	1485.00	428.00
K_0	At-rest lateral earth pressure coefficient	0.35	0.40

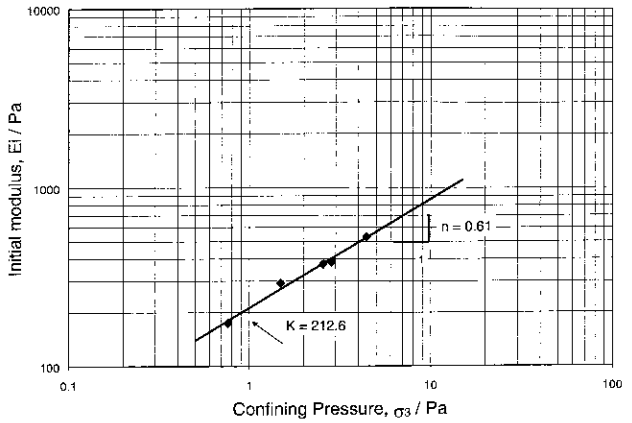

Fig. 10. Initial tangent modulus of solid waste material

scale. Based upon these results, the value of the modulus coefficient K in Eq. (1) was estimated as 212 and the value of the modulus exponent n was defined as 0.61.

Table 2 summarizes the hyperbolic parameters used to characterize the waste material in the finite element analysis, as defined from cyclic simple shear tests (stress-strain properties) and from direct shear tests (shear strength properties). The remaining parameters in Table 2 were defined based on recommendations from Duncan et al. (1980) for silts and silty clays, which constitute the soil matrix of the waste at the OII Landfill. Based upon data from the field investigation, a uniform unit weight of 15.7 kN/m^3 was used in the analyses for the solid waste material.

The native foundation material that underlies the landfill is geologically characterized as the Terciary age Pico unit of the Fernando formation. The Pico unit includes conglomerate, sandstone, and siltstone/claystone subunits. The conglomerate consists of gravels and cobbles in a silt to coarse-grained sand matrix, the sandstone contains fine- to medium-grained sand with periodic calcareous concretions, and the siltstone/claystone subunit is interlayered with fine-grained silty sandstone beds. The shear strength properties of the native foundation material, defined based on information from previous investigations (The Earth Technology Corporation, 1993; ESI, 1996), was characterized by a cohesion of 43 kPa and a friction angle of 32°. The material properties of the foundation soils were used in the finite element site response analysis performed to define the maximum average acceleration in the toe buttress area. However, since the foundation soils showed a negligible time-dependent (creep) response when compared to that of solid waste, the foundation soils were not considered in the deformation analysis that evaluated the effect of time-dependent settlements.

LIMIT EQUILIBRIUM EVALUATION OF THE TOE BUTTRESS

As the purpose of the toe buttress was to enhance the stability of slopes along the southeastern perimeter of the landfill, a stability analysis of the landfill slopes behind the toe buttress was performed. Shear strength properties of the backfill, waste, and foundation soil material were selected as described previously and are listed in Table 2. The limit equilibrium analyses were performed using Spencer's method as implemented in the program UTEXAS3 (Wright, 1990). Both circular and noncircular failure surfaces were considered. The search for the critical surface included surfaces through the near surface zone, through the waste mass, and through the bedrock. The calculated static factor of safety for the critical cross-section exceeds 2.5. This is a relatively high value, especially considering that the analyses conservatively neglected the contribution to stability provided by the concrete piers drilled along the toe buttress. The critical surfaces from these analyses passed behind the reinforced soil zone, and indicated acceptable global stability for the toe buttress.

For evaluation of the seismic stability, the yield acceleration (i.e. the pseudo-static horizontal acceleration needed to obtain a safety factor of 1.0) was calculated for the various failure modes. The calculated yield acceleration exceeds 0.45 g. This is a comparatively high value, considering that the maximum peak average horizontal acceleration for the landfill slopes behind the toe buttress is 0.48 g. This value was obtained from a finite element seismic response analysis of the entire landfill using site-specific accelerograms. Relatively high static factors of safety and pseudo-static yield accelerations were also obtained assuming the presence of adverse liquid conditions.

Finally, conventional internal stability evaluation of the geogrid-reinforced structure yielded high factors of safety (in excess of 3.5). The geogrid tensile strength properties used in the analyses were selected as described previously. However, the adequate internal and global stability indicated by limit equilibrium analyses is only valid as far as differential settlement and/or earthquake loading do not compromise the internal integrity of the toe buttress. This is because the limit equilibrium analyses do not account for the geogrid strains induced by these loading mechanisms. Consequently, a finite element simulation was performed as described next to evaluate the internal integrity of the geogrid-reinforced toe buttress subjected to differential settlement and earthquake loads.

FINITE ELEMENT EVALUATION OF THE TOE BUTTRESS

General Modeling Considerations

A numerical finite element evaluation was undertaken to evaluate the integrity of the reinforced toe buttress subjected to the anticipated differential settlements followed by the design earthquake. The simulation was performed using the finite element code GeoFEAP developed at the University of California at Berkeley for analysis of geotechnical problems. GeoFEAP is a general, plane strain, soil-structure interaction program for static analysis of geotechnical structures including consideration of

large deformations and sequential construction. The code has also been used and validated for the case of geosynthetic-reinforced soil structures (Espinoza et al., 1995). GeoFEAP is based on the general-purpose finite element program FEAP, which handles a wide variety of 2-D and 3-D problems, including heat transfer, solid and structural mechanics, and fluid mechanic problems. A macro-command structure was implemented in the program in order to facilitate simulation of sequential analyses, a feature that is particularly useful to simulate the construction of geotechnical structures such as excavations, embankments, and foundations. The macro-command structure is associated with the use of a set of compact and independent subprograms, each designed to compute one or just a few basic steps of the finite element simulation process.

Both material and geometric nonlinearity were considered in the analysis in order to account for the constitutive behavior of the materials and for large displacements. The strains induced in the geogrid reinforcement were modeled using three sequential analyses: (i) construction of the toe buttress, (ii) gradual development of differential settlement, and (iii) earthquake loading.

Although many of the reported finite element analyses of reinforced soil structures in the literature have evaluated the performance of structures reinforced with metallic strips and grids, several of these studies investigated the performance of structures reinforced with geosynthetics. Some of these studies have investigated the performance of hypothetical reinforced soil structures (e.g., Chalaturnyk et al., 1990; Rowe and Ho, 1997). Others have validated finite element results against field monitoring records of actual geogrid-reinforced structures (e.g., Adib, 1988; Bathurst et al., 1992; Zornberg and Mitchell, 1994). While previous numerical investigations have focused mainly on the performance of reinforced soil structures subjected to construction loads and vertical surcharges, the analyses presented herein evaluate the reinforcement strains induced by loads other than self-weight.

Since geosynthetic-reinforced soil structures are more flexible than metallic-reinforced structures, additional care is required in the determination of the appropriate mesh layout, material parameters, and analysis sequence. Finite element modeling of soil structures reinforced with planar, extensible geosynthetic reinforcements differs from the modeling of structures with inextensible metallic reinforcement (e.g., metal strips) in several ways. Some aspects of extensible reinforcements lead actually to a simpler modeling than for the case of inextensible systems:

- Geosynthetic reinforcements are generally placed in continuous sheet layers and, consequently, can be properly modeled as plane strain structural elements. This is generally not the case for inextensible reinforcements, such as steel strips or bar mats, which have a three-dimensional layout.
- While rigid facing can play an important role in the overall behavior of reinforced soil structures, the response of the more flexible geosynthetic-reinforced structures is dominated by soil and reinforcement characteristics. Selection of facing parameters becomes an even less relevant issue in the analysis of geosynthetic-reinforced soil structures built using flexible facing.

On the other hand, some aspects of extensible reinforcements lead to more complex modeling than for the case of structures reinforced using inextensible inclusions:

- Since the reinforcement vertical spacing in geosynthetic-reinforced soil structures is generally smaller than in structures reinforced with inextensible inclusions, a finer mesh discretization is required.
- Finite element simulation of geosynthetic-reinforced structures is more sensitive to the stress-strain-strength behavior of the backfill soil than for the case of structures reinforced with inextensible reinforcement. The comparatively stiffer reinforcement and facing components used in structures reinforced with inextensible inclusions tend to dominate the structure response.
- The effect of confinement and time on the tensile strength and stiffness of geosynthetics, particularly geotextiles, is not fully understood. Reinforcement mechanical properties, typically obtained by testing unconfined geosynthetic specimens under comparatively high strain rates, are not necessarily representative of in-service conditions.
- The backfill material undergoes larger lateral deformations in geosynthetic-reinforced soil structures than in structures reinforced with inextensible elements. Consequently, zones of highly mobilized soil shear stresses may develop within the reinforced backfill. However, the presence of highly mobilized shear stresses would not necessarily lead to a failure mechanism within the reinforced soil structure, unless the reinforcement elements have also reached their ultimate tensile strength.

Figure 11 shows the finite element mesh used in the toe buttress analyses, which was developed taking into account the general modeling considerations mentioned above. This finite element mesh consists of 1082 nodes, 1028 plane strain elements for representation of soil and waste, and 140 bar elements for simulation of the reinforcements. The final mesh layout was selected based on a sensitivity study that evaluated the numerical errors by using increasingly refined finite element meshes. Use of a relatively fine mesh discretization between reinforcement layers was found to be essential for proper representation of the soil layers. As will be discussed later, the numerical simulation involved imposing displacements at the base of the reinforced soil structure. Consequently, no elements were used to simulate the foundation soil and piers below the toe buttress structure. It should be noted, though, that the finite element mesh used in the seismic response analysis performed to define the maximum average acceleration in the toe buttress area included the waste prism and the foundation material.

The reinforcement was modeled using bar elements.

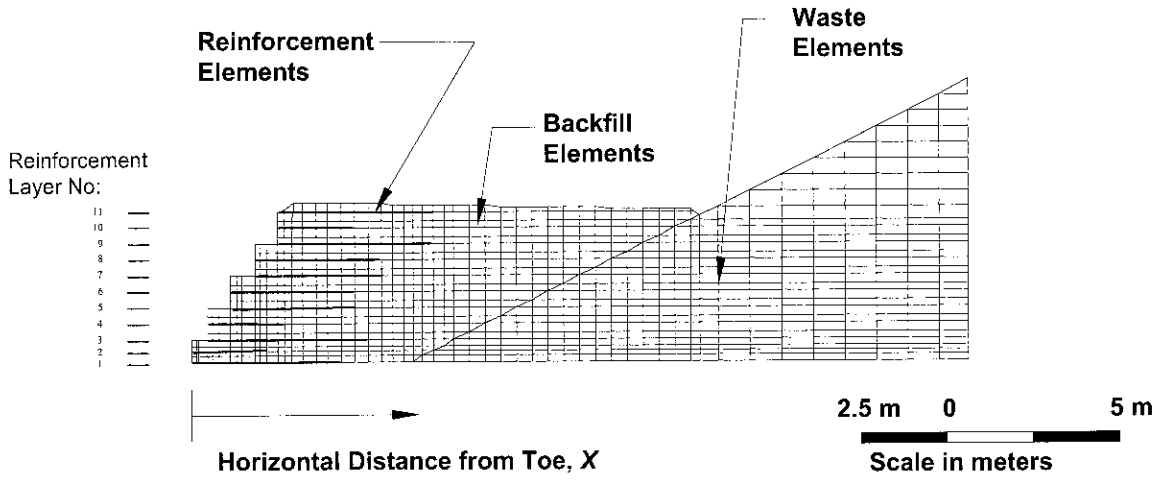

Fig. 11. Finite element mesh used in analysis of the toe buttress

The stiffness of the geogrid reinforcement was defined from the geogrid test results described previously. A stiffness of 300 kN/m was used to characterize the tensile-load strain relationship of the geogrid reinforcement during static loading. This value was obtained from the isochronous load-strain curve for 10^6 hours shown in Fig. 7. A geogrid stiffness of 425 kN/m was used to characterize the tensile load-strain relationship of the geogrids during rapid (seismic) loading. The isochronous load-strain curve for 10^0 hours (1 hour) shown in Fig. 7 was used in this case. As previously discussed, the hyperbolic model (Duncan et al., 1980) was used to characterize the stress-strain-strength behavior of the backfill soil and of the solid waste. GeoFEAP includes zero thickness interface elements capable of representing interface conditions by modeling relative movement between soil and a structure. However, the use of interface elements incorporates additional degrees of freedom in the analysis. Since a parametric study showed that the use of interface elements had only minor influence on the results, compatibility of displacements was assumed between the backfill and the reinforcement. The assumption of displacement compatibility between soil and reinforcement is justified by the high geogrid-soil interface shear strength and by the fact that geogrids can tolerate the same or greater level of strain as soil prior to failure.

Phase 1: Simulation of Toe Buttress Construction

Soil and bar elements in the reinforced soil zone were sequentially activated in order to model the construction of the toe buttress (Fig. 12). Backfill elements activated for each stage in the simulation correspond to a 0.46 m thick compacted soil layer. A sensitivity evaluation showed this to be an appropriate sequence. The self-weight load in each of the stages was added in ten load increments, and the displacements and stresses for each increment were solved using a Modified Newton-Raphson iterative approach. Vertical displacements were constrained at the base of the reinforced soil structure during this phase of the numerical simulation. Reinforcement

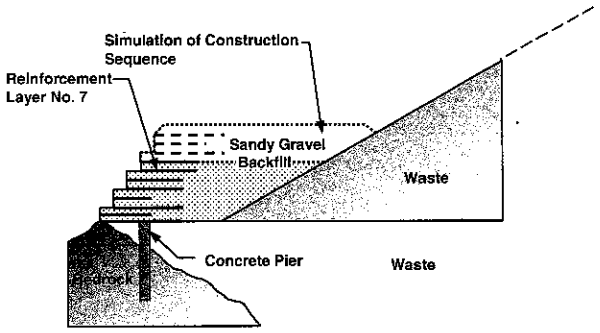

Fig. 12. Finite element simulation of the toe buttress construction

tensile strains, induced during construction by the self-weight of the backfill material, were obtained as part of these analyses.

The maximum reinforcement strain estimated in the construction simulation phase of the analysis occurs in Reinforcement Layer 7, located 2.7 m above the base of the 4.6 m high reinforced slope. The location of the maximum tension in the reinforcements is consistent with the results of a centrifuge investigation on the performance of reinforced soil slopes at failure (Zornberg et al., 1998). That study indicated that the location of the maximum tension in a reinforced soil structure depends on the inclination of the slope facing and it would be located approximately at midheight of the reinforced slope under investigation. The magnitude of geogrid strains developed during construction is comparatively small, with a maximum strain of less than 0.4%. Such a low reinforcement strain level at the end of construction is consistent with previous experience gathered from instrumented geosynthetic-reinforced slopes (e.g., Christopher et al., 1994). Figure 13 shows the strain distribution computed in Reinforcement Layer 7 during the different stages of construction of the toe buttress. The different stages indicated in this figure correspond to the number of soil layers placed during the construction simulation.

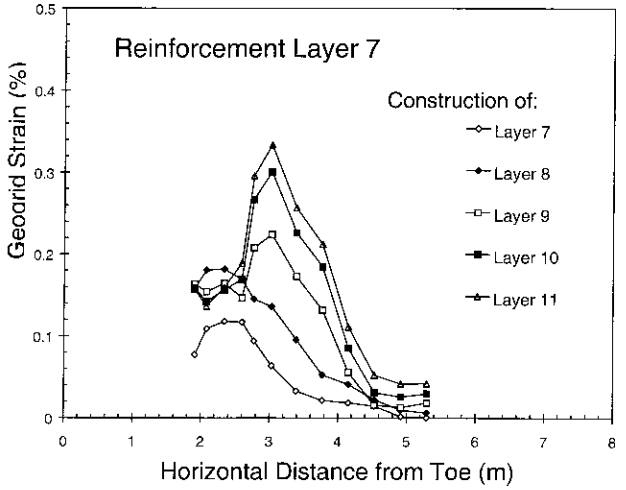

Fig. 13. Estimated geogrid strains induced during construction

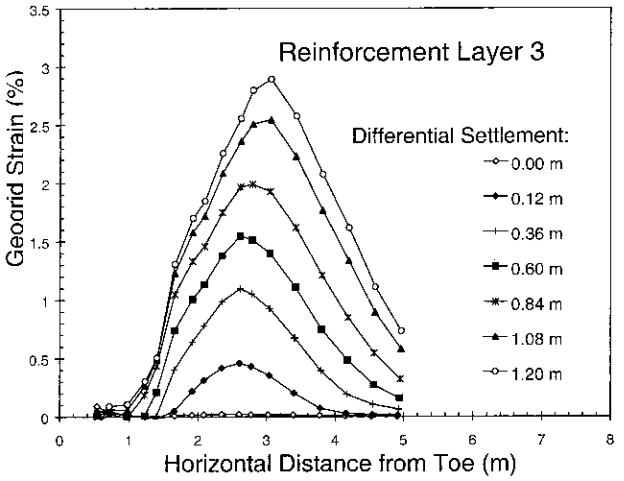

Fig. 15. Estimated geogrid strains induced by increasing differential settlements

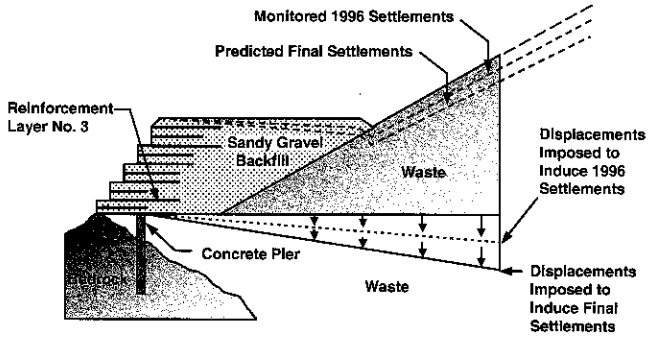

Fig. 14. Finite element simulation of the differential settlements in the toe buttress

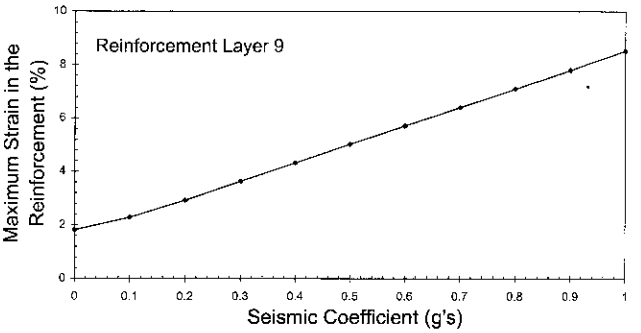

Fig. 16. Maximum estimated geogrid strains as a function of differential settlement on the surface of the toe buttress

Phase 2: Simulation of Differential Settlements

Differential settlements were imposed at the base of the reinforced soil mass during the second phase of the finite element modeling of the toe buttress (Fig. 14). Strain and tension in the reinforcements were induced by progressively increasing the base settlements in a triangular pattern, with zero settlement towards the front of the mesh and the maximum settlement at the back of the finite element mesh. A triangular settlement pattern was assumed at the base of the reinforced soil structure because: (i) settlements at the location of the concrete piers could be assumed to be negligible; (ii) settlements should be proportional to the thickness of the waste under the toe buttress, which was found to increase linearly in the vicinity of the toe buttress (from the front to the back of the structure); and (iii) a triangular settlement pattern at the base of the structure is consistent with field observations gathered after exposing the top geogrid layers.

A differential settlement of 2,000 mm was imposed at the base of the finite element mesh to simulate a long-term differential settlement of 1,200 mm on the surface of the toe buttress. The largest reinforcement strains predicted in this stage of the analysis occur towards the base of the structure. Specifically, the maximum geogrid strain computed after imposing the differential settlements occurs in Reinforcement Layer 3, located 0.9 m above the base of the toe buttress. Figure 15 shows the strain distribution estimated at this reinforcement level for increasing differential settlements.

The average differential settlement was approximately 600 mm at the time of the finite element investigation. From the results shown in Fig. 15, the maximum tensile strain in the geogrid reinforcements computed for the current condition (i.e., approximately 10 years after construction) is approximately 1.5%. In addition, Fig. 15 shows that the maximum tensile strain in the geogrid reinforcements computed for the long-term condition (i.e., after reaching 1,200 mm of differential settlements on the surface of the toe buttress) is approximately 2.9%. Both current and future geogrid strain levels induced by differential settlements, as predicted in the finite element analyses, are well below the maximum allowable static strain level of 10% established for the geogrid reinforcements.

Figure 16 shows the maximum geogrid strain plotted versus differential settlement between the front and the back of the toe buttress. The strains in the figure correspond to the maximum strain estimated in primary

Reinforcement Layer 3, located 0.9 m above the base of the toe buttress. The figure shows that the relationship between maximum geogrid strain and differential settlement is approximately linear for the range of settlements considered in the analysis. Extrapolation of the finite element results to larger strain levels indicates that approximately 3.9 m of differential settlement would be required to induce the maximum allowable static strain of 10% in the geogrids. This differential settlement exceeds by a factor of almost two the maximum long-term settlement of 1.98 m at Cross Section 3, located nearby the monitoring well shown in Fig. 3(a). As discussed previously, the settlement at this cross section was considered an outlier among the monitoring results. Following construction of the final closure system, differential settlements will be monitored in the toe buttress area as part of the post-closure monitoring plan in order to verify that they do not exceed the maximum projected values.

Phase 3: Simulation of Earthquake Loading

A seismic response analysis of the entire landfill was performed as part of the overall site investigation. This study, performed using two-dimensional equivalent-linear time domain response analyses, led to determination of the maximum average acceleration in the toe buttress area. The definition of cyclic characteristics (modulus reduction and damping curves) for the OII solid waste and the procedures used in the seismic response analysis have been described by Matasovic and Kavazanjian (1998). Seismic design of the OII Landfill was based upon a moment magnitude 6.9 earthquake on a blind thrust fault at an approximate depth of 11 km directly below the site. This design earthquake was assumed to generate a free field peak horizontal ground acceleration of 0.61 g in a hypothetical bedrock outcrop at the ground surface. These pre-design seismic analyses indicated that the peak horizontal ground acceleration might be in excess of 1.0 g at the top of the waste fill in the design earthquake. Also, mainly because of the comparatively high stiffness of the toe buttress structure, the finite element site response analysis using the design earthquake yielded a comparatively high (1.0 g) maximum average acceleration at the toe buttress location. Consequently, a pseudo-static acceleration of 1.0 g was used for the toe buttress analyses presented herein.

The reinforcement strains induced in the toe buttress by the seismic loading were estimated by applying horizontal body forces to the active reinforced soil wedge (Fig. 17). Since the entire reinforced zone, waste mass, and foundation soils are subjected to horizontal accelerations during seismic loading, the entire landfill area was considered in the dynamic finite element seismic response analysis performed to define the magnitude of the pseudo-static acceleration in the toe buttress area. However, in order to estimate the geogrid strains in the subsequent numerical simulation described herein, body forces corresponding to the maximum average acceleration estimated for the toe buttress area were applied only to the active zone defined in the internal limit equilibrium

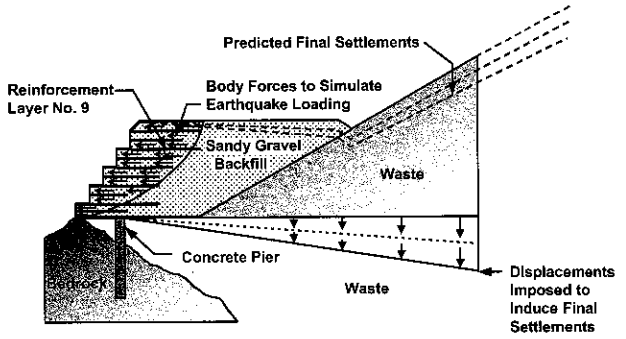

Fig. 17. Finite element simulation of earthquake loading in the toe buttress

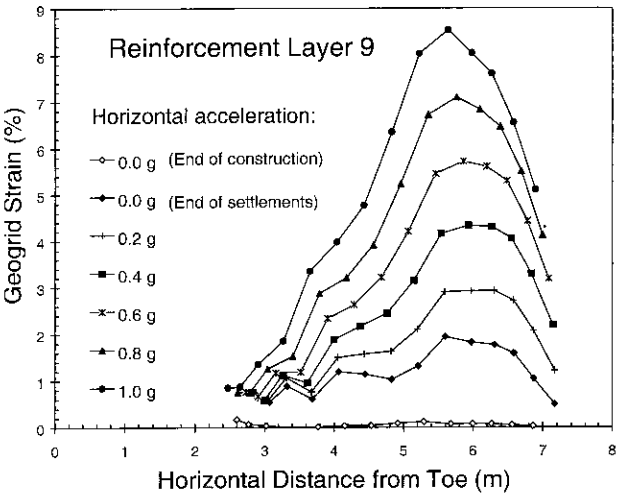

Fig. 18. Estimated geogrid strains induced by seismic loads

analysis of the structure. Applying the pseudo-static seismic load to the active zone is a conservative approximation, as the stresses induced in the reinforcements will be lower if consistent horizontal body forces were applied over the entire mesh. The use of horizontal forces in an active wedge is consistent with the pseudo-static approach used in limit equilibrium analysis of reinforced slopes (Bonaparte et al., 1986).

In contrast to the results of the previous static phases of the analysis, the location of the maximum strains induced by earthquake loading is towards the top of the reinforced soil structure. Reinforcement Layer 9, located 3.66 m above the base of the 4.6 m high toe buttress, shows the maximum estimated tensile strain when the structure is subjected to the design pseudo-static seismic loading.

The strain distribution estimated in Reinforcement Layer 9 after applying the seismically induced horizontal body forces is shown in Fig. 18. The strain distributions that correspond to the end of construction and to the long-term differential settlement are also shown in the figure (the 0.0 g cases). The final stage shown in the figure corresponds to the results obtained after applying the design earthquake loading (1.0 g). The magnitude of the

maximum tensile strain in the reinforcement at this stage of the analysis is approximately 8.5%, which is lower than the 20% allowable strain for combined static and dynamic loads. The maximum geogrid strain induced in Reinforcement Layer 9 as a function of the seismic coefficient is shown in Fig. 19. This figure shows that the relationship between the maximum incremental strain and the seismic coefficient is approximately linear for the range of seismic coefficients considered in the analysis. The 1.0 g pseudo-static seismic load induces a 6.7% strain increase in the reinforcement. Extrapolation of these results indicates that a seismic coefficient of more than 1.5 g would be required to induce an incremental strain of 10% in the geogrids (10% is the difference between the allowable strain for rapid loading and the creep limited allowable strain).

Remarks on the Numerical Simulation Results

Figure 20 summarizes the strain distribution in the five primary reinforcement layers of the toe buttress obtained after each of the three sequential phases of the analysis. This figure shows the strain distribution obtained at the end of construction, after imposing foundation differential settlements leading to approximately 600 mm of settlement at the back of the toe buttress (current condition), after imposing foundation settlements of approximately 1,220 mm at the back of the toe buttress (long-term static condition), and after applying a pseudo-static earthquake loading of 1.0 g. The maximum strain after the long-term static loading is less than 3.0%, which is well below the allowable strain for this condition of 10%. The maximum strain after applying the earthquake loading is approximately 8.5%, which is also well below the allowable combined strain of 20% for static and dynamic loading.

As shown by the numerical results obtained in the three phases of the finite element analyses, the maximum geogrid strain induced during the different phases of the study does not occur at the same elevation. Identification of the elevation at which the maximum reinforcement tension occurs may have significant impact in design. The results of the finite element analyses presented herein indicate that the maximum strain induced by construction loading occurs at midheight of the reinforced toe buttress, that the maximum strain due to differential settlement occurs towards the base of the structure, and that the maximum strain induced by earthquake loading occurs towards the top of the toe buttress. For the specific structure evaluated in this study, the analyses show that the integrity of the toe buttress at the OII Landfill should be maintained even when subjected to the projected long-term differential settlement followed by the design earth-

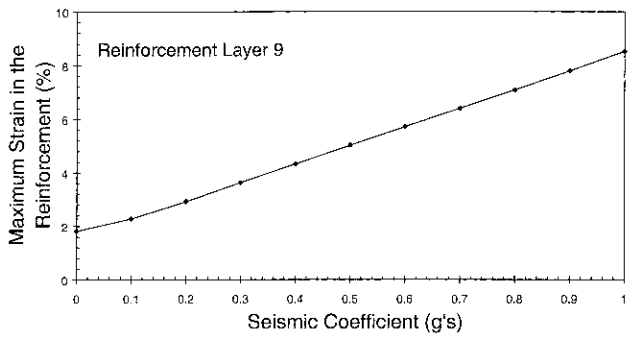

Fig. 19. Maximum estimated geogrid strain as a function of seismic coefficient

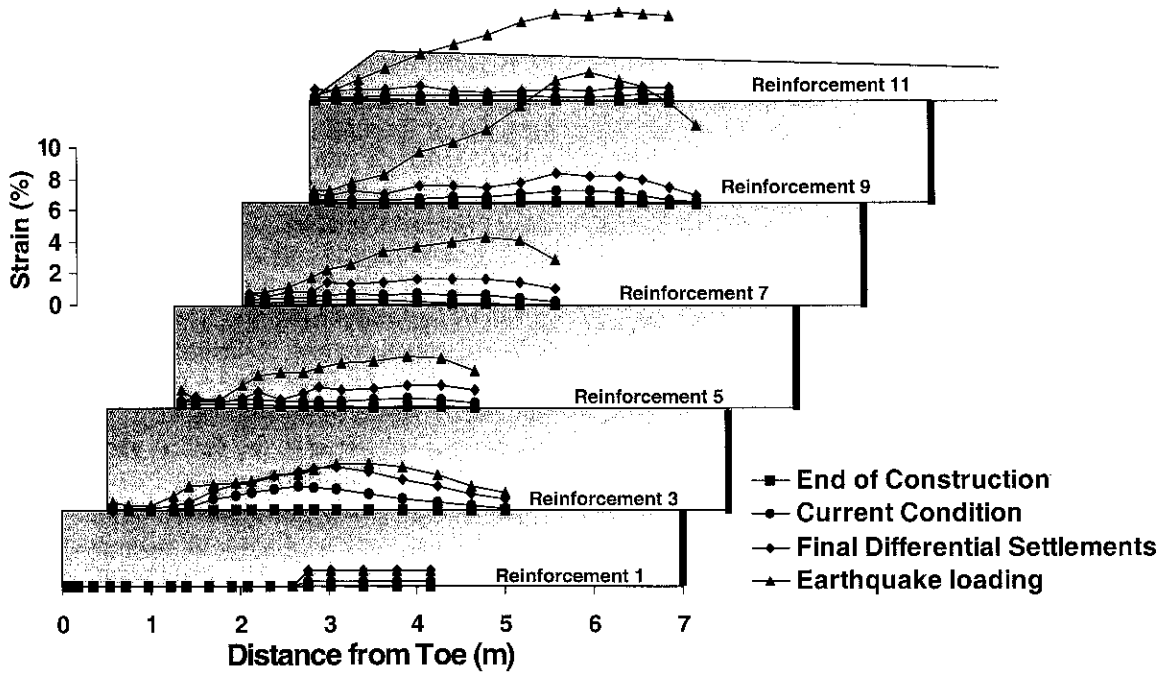

Fig. 20. Estimated geogrid strains in the toe buttress wall (Note: Vertical scale is shown only for one of the reinforcement layers. Scale is the same for all other layers.)

quake loads. The predicted adequate performance of the toe buttress had significant implications in the design of the final cover and the construction sequence at the site. In fact, rather than being an area of stability concern, the waste slopes behind the toe buttress became the first area in the landfill to undergo final cover construction under the Superfund closure program.

SUMMARY AND CONCLUSIONS

In order to enhance the stability of steep landfill slopes at the Operating Industries, Inc. (OII) Superfund site, a hazardous waste site in southern California, a geogrid-reinforced toe buttress was constructed under the direction of the EPA. The OII landfill is located approximately 16 km east of downtown Los Angeles, in an area of high seismicity. The 4.60 m high, 460 m long toe buttress was built in 1987 immediately adjacent to residential developments in 1987. The reinforced slope was constructed using uniaxial geogrids as reinforcement elements and sandy gravel as backfill material. The front of the structure was founded on concrete piers. However, as the back of the toe buttress was founded on waste, the structure experienced more than 600 mm of differential settlements since the end of its construction. In order to evaluate the internal stability of the reinforced soil structure, an investigation was undertaken to evaluate the long-term integrity of the geogrid reinforcements under static and seismic loads. The analyses considered 40 years of settlement followed by the design earthquake.

This investigation included an assessment of the monitored differential settlements in the toe buttress area, experimental determination of the mechanical properties of the geogrid reinforcements, evaluation using limit equilibrium analysis of the global stability of the landfill slopes behind the toe buttress (assuming that internal integrity of the toe buttress is maintained), and final assessment using nonlinear finite element analysis of the internal integrity of the toe buttress subjected to anticipated settlements followed by the design earthquake. The finite element simulation evaluated the strains induced in the geogrid reinforcement by three sequential loading phases: (i) toe buttress construction, modeled by sequentially activating soil and bar elements in the reinforced soil zone; (ii) gradual increase in differential settlements, simulated by imposing incremental displacements at the base of the reinforced soil mass; and (iii) earthquake loading, modeled by applying horizontal body forces that correspond to the maximum average acceleration estimated from a finite element site response analysis.

The following conclusions can be drawn from this investigation:

- Interpretation of the monitored differential settlements in the toe buttress area was a useful basis for evaluation of the settlement rate. A total differential settlement of approximately 1,200 mm was projected over additional 30 years, the time frame considered in this study.
- The limiting strain criteria used to assess the integrity of geosynthetic reinforcements should account for the different loading conditions. In this investigation, a 10% geogrid allowable strain was established for long-term static loading while a 20% geogrid allowable strain was defined for rapid (seismic) loading.
- An experimental testing program was performed to evaluate the mechanical properties of archived geogrid specimens. The results showed that rapid loading after an extended period of creep does not reduce the geogrid allowable strain nor the geogrid ultimate tensile strength to values smaller than those obtained from wide-width testing. Instead, geogrid tensile load-strain curves obtained by rapid loading after a period of constant (creep) loading eventually matched control curves obtained by rapid loading without creep.
- Numerical assessment of the geogrid strains induced at the OII toe buttress indicate that large differential settlement and severe earthquake loads should not compromise the integrity of the structure. The calculated maximum strain in the geogrid reinforcements induced after long-term differential settlements is less than 3.0%, which is well below the allowable static strain of 10%. Also, the calculated maximum geogrid strain induced after construction, long-term differential settlement, and earthquake loading is approximately 8.5%, which is well below the maximum allowable strain of 20% established for rapid loading.
- The location of the critical reinforced zone (i.e., the elevation of the reinforcement layer where the maximum strain takes place) in a geosynthetic-reinforced soil slope vary significantly for different loading mechanisms. The numerical simulation performed in this investigation indicates that the maximum reinforcement strain induced by construction loading occurs at mid-height of the reinforced slope, while the maximum strain induced by differential settlements occurs towards the base of the structure, and the maximum strain induced by earthquake loading occurs towards the top of the structure.

ACKNOWLEDGEMENTS

The support of New Cure Inc. (NCI), in particular of Dr. Lester LaFountain and Mr. Kenneth Hewlett, is gratefully acknowledged. The review and suggestions provided by Dr. David Espinoza of GeoSyntec Consultants as well as the contributions of the members of the Seismic Working Group organized by NCI and of the EPA Technical Review Panel are also greatly appreciated.

REFERENCES

1) Adib, M. E. (1988): Internal lateral earth pressure in earth walls, *Ph.D. Thesis*, Univ. of California, Berkeley, California.
2) Augello, A. J., Bray, J. D., Abrahamson, N. A. and Seed, R. B. (1998): Dynamic properties of solid waste based on back-analysis of OII landfill, *J. of Geotech. and Geoenvironmental Engrg. (ASCE)*, March, **124** (3), 211–222.
3) Bathurst, R. J., Wawrychuk, W. F. and Jarrett, P. M. (1988):

Laboratory investigation of two large-scale geogrid reinforced soil walls, *Proc. of NATO Workshop on the Application of Polymeric Reinforcement in Soil Retaining Structures*, Kingston, Ontario, 71–109.

4) Bathurst, R. J., Karpurapu, R. and Jarrett, P. M. (1992): Finite element analysis of a geogrid reinforced soil wall, *Grouting, Soil Improvement and Geosynthetics, ASCE*, 1213–1224.
5) Blight, G. E. and Dane, M. S. W. (1989): Deterioration of a wall complex constructed of reinforced earth, *Géotechnique*, **39** (1), 47–53.
6) Bonaparte, R., Schmertmann, G. R. and Williams, N. D. (1986): Seismic design of slopes reinforced with geogrids and geotextiles, *Proc. of Third Int. Conf. on Geotextiles*, Vienna, 273–278.
7) Bonaparte, R. and Berg, R. R. (1987): Long-term allowable tension for geosynthetic reinforcement, *Geosynthetic '87*, IFAI, New Orleans, LA, 181–192.
8) Chalaturnyk, R. J., Scott, J. D., Chan, D. H. K. and Richards, E. A. (1990): Stresses and deformations in a reinforced soil slope, *Can. Geotech. J.*, **27**, 224–232.
9) Chang, J. C. and Forsyth, R. F. (1977): Finite element analysis of reinforced earth wall, *ASCE J. of the Geotech. Engrg. Div.*, **103** (GT7), 677–692.
10) Christopher, B., Bonczkiewicz, C. and Holtz, R. (1994): Design, construction and monitoring of full scale test of reinforced soil walls and slopes, *Recent Case Histories of Permanent Geosynthetic-Reinforced Soil Retaining Walls*, (ed. by Tatsuoka, F. and Leshchinsky, D.), A. A. Balkema, Tokyo, Japan, 45–60.
11) Collin, J., Chouery-Curtis, V. and Berg, R. R. (1992): Field observation of reinforced soil structures under seismic loading, *Proc. of Earth Reinforcement Practice*, (ed. by Ochiai, H., Hayashi, S. and Otani, J.), A. A. Balkema, Fukuoka, Japan, 223–228.
12) Duncan, J. M., Byrne, P., Wong, K. S. and Mabry, P. (1980): Strength, stress-strain and bulk modulus parameters for finite element analyses of stresses and movements in soil masses, *Geotech. Research Report UCB/GT/80-01*, Univ. of California, Berkeley, California.
13) Elias, V. and Christopher, B. R. (1997): *Mechanically Stabilized Earth Walls and Reinforced Soil Slopes, Design and Construction Guidelines*, Department of Transportation, FHWA, Washington D. C.
14) ESI (1996): *Prefinal (90%) Predesign Report-OII Landfill, CD-3 Activities*, Report prepared for New Cure, Inc. by Environmental Solutions, Inc., February 1996.
15) Espinoza, R. D., Taylor, R. L., Bray, J. D., Soga, K., Lok, T., Rathje, E. M., Zornberg, J. G. and Lazarte, C. A. (1995): GeoFEAP: Geotech. Finite Element Analysis Program. PART I-User's Guide, *Geotech. Research Report* (UCB/GT/95-02), October 1995, Department of Civil and Environmental Eng. Univ. of California, Berkeley, California.
16) GeoSyntec Consultants (1996): *Summary Report of Findings, Report no. SWP-9*, Operating Industries, Inc. Landfill, Monterey Park, California, Prepared for New Cure, Inc.
17) Huang, C. (2000): Investigations of soil retaining structures damaged during the Chi-Chi (Taiwan) earthquake, *J. of the Chinese Institute of Engineers*, **23** (4), 417–428.
18) Huang, C. and Tatsuoka, F. (2001): Stability analysis of the geosynthetic-reinforced modular block walls damaged during the Chi-Chi earthquake, *Proc. Fourth Int. Conf. on Recent Advances in Geotech. Earthquake Engrg. and Soil Dynamics*, San Diego, (in press).
19) Kavazanjian, E. and Mitchell, J. K. (1980): Time-dependent deformation behavior of clays, *ASCE J. of the Geotech. Engrg. Div.*, **106** (GT6), 611–630.
20) Kramer, S. L. (1996): *Geotech. Earthquake Engrg.*, Prentice Hall, Inc.
21) Matasovic, N. and Kavazanjian, E. (1998): Cyclic characterization of OII landfill solid waste, *J. of Geotech. and Geoenvironmental Engrg. (ASCE)*, **124** (3), 197–210.
22) McGown, A., Andrawes, K. Z., Yeo, K. C. and DuBois, D. D. (1984): The load-strain-time behavior of Tensar geogrids, *Polymer Grid Reinforcement in Civil Engrg.*, The Institution of Civil Engineers, London, UK, 11–17.
23) Morochnik, V., Bardet, J. P. and Hushmand, B. (1998): Identification of dynamic properties of OII landfill, *J. of Geotech. and Geoenvironmental Engrg. ASCE*, **124** (3), 186–196.
24) Rowe, R. K and Ho, S. K. (1997): Continuous panel reinforced soil walls on rigid foundations, *J. of Geotech. and Geoenvironmental Engrg. (ASCE)*, **123** (10), 912–920.
25) Sandri, D. (1994): Retaining walls stand up to the Northridge earthquake, *Geotech. Fabrics Report* (June/July), **12**, (4), 30–31.
26) Stevens, J. B. and Souiedan, B. (1990): Geotextile wall aids bridge construction, *Geotech. Fabrics Report*, (May/June), 10–15.
27) Stewart, J. P., Seed, R. B., Riemer, M. F. and Zornberg, J. G. (1994): Geotechnical aspects of the Northridge earthquake of January 17, 1994-Geotechnical Structures, *Geotech. News*, 59–62.
28) Tatsuoka, F., Murata, O., Tatemaya, M., Nakamura, K., Tamura, Y., Ling, H. I., Iwasaki, K. and Yamanouchi, H. (1990): Reinforcing steep clay slopes with a nonwoven geotextile, *Proc. of Int. Conf. on Performance of Reinforced Soil Structures*, (ed. by McGown, A., Yeo, K. and Andrawes, K. Z.), Thomas Telford Ltd, 141–146.
29) Tatsuoka, F., Koseki, J. and Tatemaya, M. (1996): Performance of reinforced soil structures during the 1995 Hyogo-ken Nanbu Earthquake, Special report, *Proc. of Int. Symp. on Earth Reinforcement* (ed. by Ochiai, H., Yasufuku, N. and Omine, K.), IS Kyushu '96, **2**, 105–140.
30) Tatsuoka, F., Koseki, J., Tatemaya, M., Munaf, Y. and Khan, A. J. (1998): Seismic stability against high seismic loads of geosynthetic-reinforced soil retaining structures, Keynote Lecture, *Proc. of Sixth Int. Conf. on Geosynthetics*, Atlanta, Georgia, **1**, 103–142.
31) The Earth Technology Corporation (1993): *Geotechnical Investigation for the Proposed Expansion Area at the Puente Hills Landfill. Volume I*, Prepared for County Sanitation District of Los Angeles County, September 1993.
32) White, D. M. (1996): Performance of geosynthetic-reinforced slopes and walls during the Northridge, California Earthquake of January 17, 1994, *Int. Symp. on Earth Reinforcement*, IS Kyushu '96, Fukuoka, Japan, **2**, 97–104.
33) Woodward Clyde Consultants (1986): Final slope stability report of initial remedial measures, remedial investigation, and feasibility study for Operating Industries, Inc., *Landfill Site, Document Control* (120-WP2-RT-BJPR-2).
34) Woodward Clyde Consultants (1987): Completion report-Construction observation and tests, South toe buttress, Operating Industries, Inc., *Landfill, Monterey Park, California, Completion Report to US EPA Region IX*.
35) Wright, S. G. (1990): *UTEXAS3 A Computer Program for Slope Stability Calculations*, Austin, Texas.
36) Zornberg, J. G. and Mitchell, J. K. (1994): Finite element prediction of the performance of an instrumented geotextile-reinforced wall, *Proc. of Eight Int. Conf. of the Int. Association for Computer Methods and Advances in Geomechanics* (IACMAG '94), **2**, Morgantown, WV, 1433–1438.
37) Zornberg, J. G. and Caldwell, J. A. (1998): Design of monocovers for landfills in arid locations, *Proc. of Third Int. Conf. on Environmental Geotechnics*, (ed. by Secoe Pinto, P. S.), Lisbon, Portugal, September 1998, A. A. Balkema, **1**, 169–174.
38) Zornberg, J. G. and Kavazanjian Jr., E. (1998): Evaluation of a geogrid-reinforced slope subjected to differential settlements, *Proc. of Sixth Int. Conf. on Geosynthetics*, Atlanta, Georgia, (1), 469–474.
39) Zornberg, J. G., Sitar, N. and Mitchell, J. K. (1998): Performance of geosynthetic reinforced slopes at failure, *J. of Geotech. and Geoenvironmental Engrg. ASCE*, **124** (8), 670–683.